IEICE Communications Express, Vol.13, No.4, 110–113

ComEX

LETTER

Delay analysis of UAV networks with hybrid wireless and power line communication

Liangbin Zhu[1, a)], **Qinghai Yang**[2], **and Shuman Ding**[2]

Abstract The unmanned aerial vehicle (UAV) network has been widely studied for for various metrics, e.g., flexible and reliable. Among these metrics, delay is a major performance metric for UAV network. This paper models a UAV network with hybrid wirless and power line communication (PLC) where data is first relayed through a wireless channel and then transmitted through a PLC system. We analysis the delay performance of the hybrid network via SNC approach. Numerical results shows how various parameters affect the delay performance under the service capability derived.

Keywords: UAV network, PLC, SNC, delay analysis
Classification: Wireless communication technologies

1. Introduction

Unmanned Aerial Vehicle (UAV) networks are attracting increasing attention in recent years. UAVs can be rapidly deployed to meet the needs of various applications, such as search and rescue, surveillance, and communication relay. In some of these missions such as disaster monitoring and military applications, ensuring continuous network services poses a significant challenge, particularly when drones are required to sustain tasks such as target detection and data transmission over extended durations without reliable, continuous power sources. Faced with the above challenge, the power line communication (PLC) is introduced into the UAV network, which is able to ensure power supply and improve transmission performance. Despite these advantages, the complexity of PLC additive noise makes it difficult to describe, since it is a mixture of background noise and pulse noise. It can be described by the Nakagami-m distribution and middleton class A distribution [1]. The Bernoulli-Gaussian distributions is also widely used in the literature to model both types of noise. The multiplicative noise can be well described by Rician fading model and Rayleigh fading model [2], and the Log-normal distribution is an excellent model for PLC [3]. In response to the problems raised above, the stochastic network calculus (SNC) [4] in the signal-to-noise-ratio (SNR) domain is used to capture the service capability of wireless channels, how to integrate PLC into modern communication and model channels of UAV networks is still a huge challenge.

In this paper, a wireless-PLC hybrid UAV network is modeled by using Poisson point process (PPP), and the statistical characteristics of the service incremental processes of both channels are analyzed. To address the delay analysis in a wireless-PLC hybrid network, we contemplate the SNC as a prospective solution method. The use of the convolution operator in SNC allows us to analyze the delay of series queues, providing convenience to evaluate the performance of hybrid network. Hence, the SNC approach is used to analyse the delay performance.

2. Network model

In this scenario, we consider a multi-cluster UAV network, where relay drones establish power connections via power lines to ensure a continuous power supply while extending the surveillance range. Simultaneously, source drones, responsible for the surveillance mission, are randomly distributed within the same plane as relay drones and communicate with them via wireless channels. It is a wireless-PLC hybrid network model that data is first sent from the source to the relay through a wireless channel and the data is then transmitted to the destination over PLC link, as shown in Fig. 1. In such network, we use PPP to describe the spatial position of communication equipments. In particular, we use a homogeneous PPP to model the location of the active sources, that is, $\Phi_{\mathbf{T}} = \{x_i\}$ with density λ, where $x_i \in \mathbb{R}^2$ for $\forall i \in \{1, \ldots, N\}$ represents the location of sources. Once the destination reaches its designated location $x_0 \in \mathbb{R}^2$, it releases a UAV equipped with a power cable to facilitate the continuous power supply of this UAV and the data communication between them. And we focus on a transmission pair between a typical receiver at the origin and its corresponding transmitter at x_0.

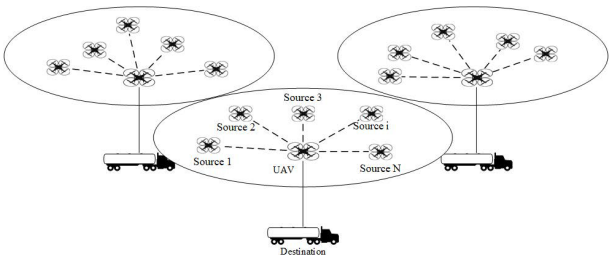

Fig. 1 A UAV network with wireless and power line communication.

[1] School of Information and Electronics, Beijing Institute of Technology, Beijing, 100000, China
[2] School of Telecommunications Engineering, Xidian University, Xi'an, 710071, China
[a)] zhuliangbin042471@163.com

DOI: 10.23919/comex.2023XBL0169
Received November 30, 2023
Accepted December 20, 2023
Publicized February 16, 2024
Copyedited April 1, 2024

2.1 Wireless link

To evaluate the service capabilities of wireless links, we adopt the path loss propagation model with path loss index $\alpha > 2$ and Rayleigh channel fading. The channel fading coefficient remains static within each time slot and independent of each other, showing an exponential distribution with an average value of 1. For simplicity, we assume that all sources have a fixed transmit power P, and thus the signal received signal power of UAV is $Ph(t)r_i^{-\alpha}$, where $h(t)$ is the instantaneous Rayleigh fading gain and r_i is the distance between source i and UAV.

In the depicted scenario, intra-cluster drones employ frequency division orthogonality. During the uplink phase, when all intra-cluster users simultaneously transmit information, co-channel interference arises from adjacent cluster UAVs transmitting on the same frequency. We focus on the interference, which is described as the cumulative signal power from all other transmitter ambient. The noise power is denoted as σ^2 for analysis integrity. H is the flight altitude of the UAVs. The instantaneous SNR of the wireless link is

$$\gamma_w(t) = \frac{Ph(t)r^{-\alpha}}{\sum_{X_i \in \Phi_{\mathbf{T}} \setminus x_0} Pw_i(t)||x_i||^{-\alpha} + \sigma^2}, \tag{1}$$

where $w_i(t)$ is the Rayleigh fading channel power of the interference channel.

2.2 PLC link

The Log-normal distributed channel gain and Bernoulli-Gaussian noise are used to model the PLC link. Similarly, the instantaneous SNR of a PLC link is

$$\gamma_p(t) = \frac{P_p h_p(t)}{n}, \tag{2}$$

where h_p is the PLC channel gain. For the Bernoulli-Gaussian noise, the probability distribution function (PDF) is

$$f(n) = (1-\rho)\mathcal{CN}(0, \sigma_g^2) + \rho\mathcal{CN}(0, \sigma_g^2 + \sigma_i^2). \tag{3}$$

Herein $\mathcal{CN}(0, \sigma^2)$ is the complex Gaussian distribution. ρ is the probability of the impulsive component of the Bernoulli-Gaussian noise. The background noise power of PLC link is σ_g^2. With background and impulsive noise, the total noise power is $\sigma_i^2 = \sigma_g^2(1+K)$, where $K = \sigma_i^2/\sigma_g^2$ is the impulsive noise index.

Using the above system and channel model, we further analyze the delay bound of the hybrid network through SNC in the SNR domain.

3. Delay analysis

The hybrid network is a discrete fluid flow queuing system, the arrival and service process is defined as $A(t)$ and $S(t)$ and the arrival and service increments are defined as a and s. In order to utilize SNC in the SNR domain, we convert these two factors into the exponential domain as $\mathcal{A}(t) = e^{A(t)}$ and $\mathcal{S}(t) = e^{S(t)}$. By applying Chernoff's bound $\Pr\{X(\tau,t) \geq x\} \leq x^{-\beta} M_X(1+\beta, \tau, t)$, one can readily derive the probabilistic performance bound for any nonnegative random variable (RV) X, where $M_X(\beta, \tau, t) = E[(X(\tau,t))^{\beta-1}]$ is the Mellin transform of X. With Chernoff's inequality and the Mellin transforms of arrival and service incremental processes, the delay bound can be easily computed via SNC in the SNR domain.

In this work, a data flow model of Poisson arrival process is considered, which the arrival increment is a Poisson random variable with an average δ, which is represented equivalently in the SNR domain as $M_a(\beta) = e^{\delta(e^{\beta-1}-1)}$.

Next, we evaluate the Mellin transform of the service incremental process pertaining to both wireless and PLC links. We put forward the nearest association strategy to improve channel condition. The distance distribution between the typical receiver and its closest transmitter is provided as $f_d(r) = 2\pi\lambda r \exp(-\lambda\pi r^2)$.

We will derive the Mellin transform of the service increments for the wireless link. Firstly, since there is a great distance between the interferers and the connected transmitter, the Laplace transform can be derived as the Laplace transform of cumulative interference I_r is given with parameter $s = r^\alpha P^{-1} x$ as

$$\begin{aligned} L_{I_r}(s) &= \mathbb{E}_{\Phi, w_i}\left[\exp\left(-s \sum_{x_i \in \Phi \setminus x_0} w_i P \|x_i\|^{-\alpha}\right)\right] \\ &= \exp\left(-2\pi\lambda \int_r^\infty \left(1 - \frac{1}{1+sPy^{-\alpha}}\right) y \mathrm{d}y\right). \end{aligned} \tag{4}$$

Then we focus on the statistical characteristics of λ. The CDF of λ can be written as

$$\begin{aligned} F_\gamma(x) &= 1 - \mathbb{E}_r(\exp(-r^\alpha P^{-1}\sigma^2 x)\, L_{I_r}(r^\alpha P^{-1} x)) \\ &= 1 - 2\pi\lambda \int_0^\infty \exp(-r^\alpha P^{-1}\sigma^2 x - \lambda\pi r^2) \\ &\quad \times L_{I_r}(r^\alpha P^{-1} x) r \mathrm{d}r. \end{aligned} \tag{5}$$

By taking the derivative of $F_\gamma(x)$ in Eq. (5), we can obtain the corresponding PDF $f_\gamma(x)$ as follows

$$\begin{aligned} f_\gamma(x) = &-2\pi\lambda \int_0^\infty r \exp\left(-\pi\lambda r^2 - r^\alpha P^{-1}\sigma^2 x\right) L_{I_r}\left(r^\alpha P^{-1} x\right) \\ &\times \left(-r^\alpha P^{-1} x - 2\pi\lambda \int_r^\infty \frac{r^\alpha y^{1-\alpha}}{(1+r^\alpha x y^{-\alpha})^2} \mathrm{d}y\right) \mathrm{d}r. \end{aligned} \tag{6}$$

The Mellin transform of service incremental process is

$$\begin{aligned} M_{s_w}(\beta) = 2\pi\lambda &\int_0^\infty \int_0^\infty \int_r^\infty r(1+x)^{\frac{(\beta-1)W}{\ln 2}} \\ &\times \exp\left(\pi\lambda r^2 + r^\alpha P^{-1}\sigma^2 x\right) L_{I_r}\left(r^\alpha P^{-1} x\right) \\ &\times \left(-r^\alpha P^{-1} x - 2\pi\lambda \frac{r^\alpha y^{1-\alpha}}{(1+r^\alpha x y^{-\alpha})^2}\right) \mathrm{d}y\, \mathrm{d}r\, \mathrm{d}x. \end{aligned} \tag{7}$$

The result in Eq. (7) is a triple integral, which is intricate. Therefore, we aim to simplify it. We focus on the special case that $\alpha = 4$ and $\sigma^2 = 0$ to simplify the result in Eq. (4). It can be further simplified as

$$\begin{aligned} L_{I_r}\left(r^2 P^{-1} x\right) &= \exp\left(-2\pi\lambda \int_r^\infty \frac{xy}{x + y^2 r^{-2}} \mathrm{d}y\right) \\ &\overset{(a)}{=} \exp\left(-\pi r^2 \lambda x^{\frac{1}{2}} \int_{x^{-\frac{1}{2}}}^\infty \frac{1}{1+u^2} \mathrm{d}u\right) \\ &= \exp\left(-\pi r^2 \lambda \sqrt{x} \arctan\sqrt{x}\right). \end{aligned} \tag{8}$$

where step (a) is obtained by utilizing the variable transformation $u = x^{-\frac{1}{2}} r^{-2} y^2$. With the Laplace transform under $\alpha = 4$ and $\sigma^2 = 0$, we can extend the expression for $F_\gamma(x)$ in Eq. (5) as

$$\begin{aligned} F_\gamma(x) &= 1 - \pi\lambda \int_0^\infty \exp\left(-\pi\lambda r^2 (1 + \sqrt{x}\arctan\sqrt{x})\right) \mathrm{d}r^2 \\ &= \frac{\sqrt{x}\arctan\sqrt{x}}{1 + \sqrt{x}\arctan\sqrt{x}}. \end{aligned} \tag{9}$$

In conclusion, if $\alpha = 4$ and $\sigma^2 = 0$ then the Mellin transform of service increments is

$$M_{s_w}(\beta) = \int_0^\infty \frac{(1+x)^{\frac{W(\beta-1)}{\ln 2}-1}\left((1+x)\arctan\sqrt{x} + x^2\right)}{2\sqrt{x}(1+\sqrt{x}\arctan\sqrt{x})^2}\mathrm{d}x. \tag{10}$$

We analyse the instantaneous SNR of the PLC link in two cases with pulse noise and without pulse noise which expressed as γ_p^1 and γ_p^2. If the instantaneous SNR of the PLC link only have background noise, γ_p^1 written as

$$\gamma_p^1 = \frac{|h_p|^2 P_p}{\sigma_g^2}. \tag{11}$$

Otherwise, with impulsive noise, γ_p^2 is written as

$$\gamma_p^2 = \frac{|h_p|^2 P_p}{\sigma_g^2(1+K)}. \tag{12}$$

The two RVs above are also Log-normal RVs and their PDFs are

$$f_{\gamma_p}(\gamma) = \begin{cases} f_{\gamma_p^1}(\gamma) = \frac{1}{\gamma\sqrt{2\pi 4\sigma_p^2}} \times \exp\left(-\frac{(\ln\gamma - \ln\frac{P_p}{\sigma_g^2} - 2\mu_p)^2}{8\sigma_p^2}\right), \\ f_{\gamma_p^2}(\gamma) = \frac{1}{\gamma\sqrt{2\pi 4\sigma_p^2}} \times \exp\left(-\frac{(\ln\gamma - \ln\frac{P_p}{\sigma_g^2(K+1)} - 2\mu_p)^2}{8\sigma_p^2}\right). \end{cases} \tag{13}$$

Using the above PDFs of SNRs, we can further derive the Mellin transform of the service increments of the PLC link with Shannon capacity as

$$\begin{aligned} M_{s_p}(\beta) &= E\left[(1+\gamma)^{\frac{W(\beta-1)}{\ln 2}}\right] \\ &= \int_0^\infty (1+x)^{\frac{W(\beta-1)}{\ln 2}} f_{\gamma_p}(x)\mathrm{d}x. \end{aligned} \tag{14}$$

Inserting Eq. (13) into Eq. (14), if there is only the background noise, the Mellin transform of the service incremental process of the PLC link is expressed by

$$\begin{aligned} M_{s_p}^1 = &\frac{1}{\sqrt{2\pi}2\sigma_p}\int_0^\infty \frac{(1+x)^{\frac{W(\beta-1)}{\ln 2}}}{x} \\ &\times \exp\left(-\frac{(\ln x - \ln\frac{P_p}{\sigma_g^2} - 2\mu_p)^2}{8\sigma_p^2}\right)\mathrm{d}x. \end{aligned} \tag{15}$$

In another case, we consider the impulsive noise for the PLC link, the Mellin transform of the service incremental process can be written as

$$\begin{aligned} M_{s_p}^2 = &\frac{1}{\sqrt{2\pi}2\sigma_p}\int_0^\infty \frac{(1+x)^{\frac{W(\beta-1)}{\ln 2}}}{x} \\ &\times \exp\left(-\frac{(\ln x - \ln\frac{P_p}{\sigma_g^2(K+1)} - 2\mu_p)^2}{8\sigma_p^2}\right)\mathrm{d}x. \end{aligned} \tag{16}$$

With the independent property of the Mellin transform, the analytical average delay bound of the PLC link is

$$M_{s_p} = (1-\rho)M_{s_p}^1 + \rho M_{s_p}^2. \tag{17}$$

Finally, the channel capacity is transformed into the SNR domain and Mellin transform of service increment is written by

$$\begin{aligned} M_{s_w}(\beta) &= \mathbb{E}\left[(1+\gamma_w)^{\frac{(\beta-1)W}{\ln 2}}\right] \\ &= \int_0^\infty (1+x)^{\frac{(\beta-1)W}{\ln 2}} f_\gamma(x)\mathrm{d}x \\ &= \int_0^\infty (1+x)^{\frac{(\beta-1)W}{\ln 2}} \left(r^\alpha P^{-1}\sigma^2 + 4\lambda\pi^2 r^2 x^{\frac{2}{\alpha}-1}\left(\alpha^2 \sin\frac{2\pi}{\alpha}\right)^{-1}\right) \\ &\quad \times \exp\left(-r^\alpha P^{-1}\sigma^2 x - 2\lambda\pi^2 r^2 x^{\frac{2}{\alpha}}\left(\alpha\sin\frac{2\pi}{\alpha}\right)^{-1}\right)\mathrm{d}x. \end{aligned} \tag{18}$$

Therefore, the delay bound of these two queues for any random traffic is easily calculated. By using the convolution operator of min-plus algebra in SNC, the two-stage tandem queue is equivalent to a single queue whose Mellin transform is

$$\begin{aligned} M_{\mathcal{S}_{overall}}(\beta,\tau,t) &= M_{s_w \otimes s_p}(\beta,\tau,t) \\ &\le \sum_{u=\tau}^{t} M_{s_w}(\beta,\tau,u)\cdot M_{s_p}(\beta,u,t) \\ &= \frac{M_{s_p}^{t-\tau}(\beta) - M_{s_w}^{t-\tau+1}(\beta)M_{s_p}^{-1}(\beta)}{1 - M_{s_w}(\beta)M_{s_p}^{-1}(\beta)}, \end{aligned} \tag{19}$$

where $\otimes$ and $\oslash$ are convolution operator and deconvolution operator defined in [5]. Then the delay bound is derived by

$$\begin{aligned} &\Pr\{W(t) > w\} \le \Pr\{\mathcal{A} \oslash \mathcal{S}_{overall}(t, t+w) > 1\} \\ &\le \lim_{t\to\infty}\sum_{u=0}^{t} M_{\mathcal{A}}(1+\beta,u,t) \times M_{\mathcal{S}_{overall}}(1-\beta,u,t+w) \\ &\le \lim_{t\to\infty}\Bigg[\sum_{u=0}^{t} M_a^{t-u}(1+\beta)M_{s_p}^{t+w-u}(1-\beta) - M_{s_p}^{-1}(1-\beta)M_a^{t-u} \\ &\qquad (1+\beta)M_{s_w}^{t+w-u+1}(1-\beta)\Bigg] \Big/ \left(1 - M_{s_w}(1-\beta)M_{s_p}^{-1}(1-\beta)\right) \\ &= \frac{1}{1 - M_{s_1}(1-\beta)M_{s_2}^{-1}(1-\beta)} \times \Bigg[\frac{M_{s_2}^w(1-\beta)}{1 - M_a(1+\beta)M_{s_2}(1-\beta)} \\ &\qquad - \frac{M_{s_2}^{-1}(1-\theta)M_{s_1}^{w+1}(1-\beta)}{1 - M_a(1+\beta)\,M_{s_1}(1-\beta)}\Bigg]. \end{aligned} \tag{20}$$

Note that the first inequality is based on the property that for a single queue with arrival $\mathcal{A}$ and service $\mathcal{S}$ in the SNR domain, the delay bound can be expressed as $W(t) = \inf\{u \ge 0 : \mathcal{A} \oslash \mathcal{S}(t, t+u) \le 1\}$.

4. Numerical results

In Fig. 2, we explore how the delay bound is affected by variations in both δ and $\frac{P}{\sigma^2}$ across different levels of delay violation probability. We maintain other parameters at fixed values: $B = \ln 2$ MHz, $\rho = 0.8$, $K = 30$, and $\frac{P_p}{\sigma_g^2} = 7$ dB. As δ increases, the delay bound deteriorates due to a greater influx of traffic, resulting in increased queue congestion. Conversely, a higher SNR value for $\frac{P_p}{\sigma_g^2}$ signifies a more favorable transmission environment and a reduced delay bound.

Figure 3 illustrates how the delay bound versus varies with average SNR of the PLC link, considering various values of K and ρ. For this, δ is kept constant at 100 kbps. The average SNR of the wireless link is set to $\frac{P}{\sigma^2} = 5$ dB. For the PLC link, we maintain parameters $\mu_{h_p} = 1$ and $\sigma_{h_p}^2 = 1$. The results show that the delay bound deteriorates significantly as K increases. As K grows, the service capability becomes weaker in the presence of impulsive noise, as indicated by Eq. (9) and Eq. (10). This results in an overall reduction in service capability and leads to an increase in the delay bound.

Regarding additional parameters such as data rate (δ) and the average SNR (P_p/σ_g^2), their effects on system performance can also be assessed using Figs. 2 and 3. The delay bound increases with the increase of data rate. It is reasonable since a higher data rate means more traffic congestion, which results in higher delay level.

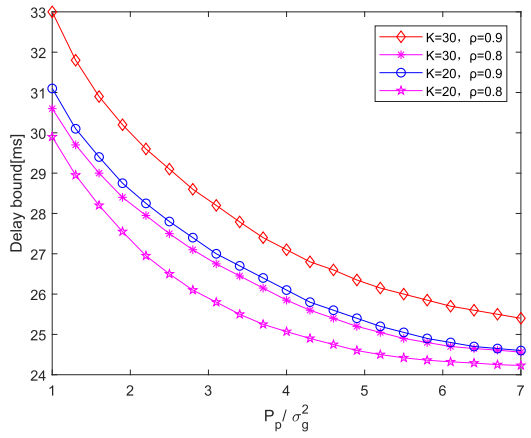

Fig. 2 Delay versus P_p/σ_g^2 under various PLC channel.

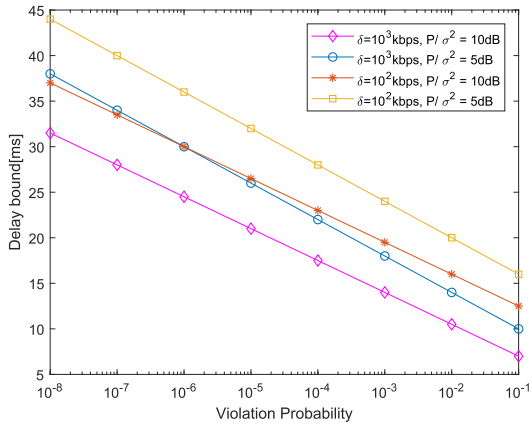

Fig. 3 Delay versus violation probability under various data flow and P/σ^2.

5. Conclusion

The paper models a hybrid wireless-PLC UAV network using a two-stage tandem queue. The delay bound for this UAV network is derived by SNC in the SNR domain. The numerical results demonstrate the impact of various factors and provide insight for network deployment and flow control for hybrid networks under different delay requirements.

References

[1] R. Wang, H. Fang, Y. Zhang, L. Yu, and J. Chen, "Low-rank enforced fault feature extraction of rolling bearings in a complex noisy environment: A perspective of statistical modeling of noises," *IEEE Trans. Instrum. Meas.*, vol. 71, pp. 1–14, April 2022. DOI: 10.1109/TIM.2022.3165281

[2] L. Yang, X. Yan, S. Li, D.B. da Costa, and M.-S. Alouini, "Performance analysis of dual-hop mixed PLC/RF communication systems," *IEEE Syst. J.*, vol. 16, no. 2, pp. 2867–2878, June 2022. DOI: 10.1109/JSYST.2021.3088096

[3] M. Yang, S. Shahramian, H. Shakiba, H. Wong, P. Krotnev, and A.C. Carusone, "Statistical BER analysis of wireline links with non-binary linear block codes subject to DFE error propagation," *IEEE Trans. Circuits Syst. I, Reg. Papers*, vol. 67, no. 1, pp. 284–297, Jan. 2020. DOI: 10.1109/TCSI.2019.2943569

[4] Y. Han, M. Yao, Y. Yang, Y. Luo, and L. XueFang, "Improving scalability of delay bound with stochastic network calculus," IEEE Global Communications Conference, IEEE GLOBECOM, Taipei, Taiwan, pp. 1–6, Dec. 2020. DOI: 10.1109/GLOBECOM42002.2020.9322552

[5] H. Al-Zubaidy, J. Liebeherr, and A. Burchard, "Network-layer performance analysis of multihop fading channels," *IEEE/ACM Trans. Netw.*, vol. 24, no. 1, pp. 204–217, Feb. 2016. DOI: 10.1109/TNET.2014.2360675